Journal of Atmospheric Chemistry **12**: 287–298, 1991.

High Resolution Spectral Features of a Series of Aromatic Hydrocarbons and BrO: Potential Interferences in Atmospheric OH-Measurements

R. NEUROTH, H.-P. DORN, and U. PLATT *
Institut für Chemie 3, Forschungszentrum Jülich, D-5170 Jülich, Germany

(Received: 18 June 1990)

Abstract. Naphthalene ($C_{10}H_8$), several other hydrocarbons, mostly derivates of naphthalene, and bromine oxide (BrO) were analyzed for narrow band ($\leqslant$0.01 nm) absorption lines in the wavelength range between 307.7 and 308.3 nm to study their potential impact on OH radical measurements by differential absorption spectroscopy.

Only naphthalene showed narrow band absorption lines in this wavelength region. From nine naphthalene lines the differential absorption cross-section σ' was determined.

The strongest naphthalene line at 308.002 nm is close to the $Q_1(2)$ OH line, but about a factor of 200 weaker ($\sigma' = (65.2 \pm 15.3) \times 10^{-20}$ cm^2/molec). The corresponding detection limit for naphthalene is about 15 ppt. We re-evaluated some spectra of our OH measurement campaign in July 1987 with respect to naphthalene and obtained an upper limit of 30 ppt for its concentration.

BrO was recorded in the larger wavelength interval between 307.7 and 308.7 nm. Structured absorptions were only observed at wavelengths above 308.2 nm and no significant structures were found in the vicinity of the $Q_1(2)$ and $Q_1(3)$ OH lines.

Key words: Naphthalene, bromine oxide, differential absorption spectroscopy, OH measurement, interferences.

1. Introduction

The measurement of atmospheric OH concentrations by long-path absorption spectroscopy (LPAS) is disturbed by the presence of overlapping absorption structures due to certain other atmosheric species. Of those, SO_2, CS_2, and HCHO were identified during the development of the LPAS technique (Hübler *et al.*, 1984). While the differential fine structure of these absorbers is several orders of magnitude weaker ($\sigma' \approx 10^{-21}$ cm^2) than that of OH ($\sigma' \approx 10^{-16}$ cm^2) (Callies, 1988), the concentration of the interfering species is – at least in polluted air – many orders of magnitude higher. Thus, the absorption lines of interfering species can be of comparable strength to those of OH. In addition, a number of lines were repeatedly observed which could not yet be assigned to atmospheric molecules. This paper describes another attempt at such identification by investigating naphthalene, several other hydrocarbons, mostly derivates of naphthalene, and bromine oxide.

* Present address: Inst. für Umweltphysik, Univ. Heidelberg, INF 366, D-6900 Heidelberg, Germany.

2. Experimental

The measurements were carried out with the same spectrograph as used in atmospheric OH measurements (for details, see Callies *et al.* (1988) and Dorn *et al.* (1988)).

Instead of the laser light source a xenon high pressure arc lamp (Canrad Hanovia 959 C 1980, 500 W) was used. After passing a long quartz cell the light was focussed on the entrance slit of the spectrograph (Czerny Turner double monochromator, modified version of the SPEX 1402), which was operated in second order with a linear dispersion of 0.136 nm/mm. The resolution was 1.8×10^{-3} nm at an entrance slit width of 12 μm (Callies, 1988).

The spectra were recorded with a linear photodiode array (PDA), Reticon RL 1024S. In order to adapt the dispersion of the spectrograph to the dimensions of the PDA, the spectrum was expanded by about a factor of 11 with a plano-convex quartz lens. Thus, the smallest just resolvable wavelength interval of 1.8×10^{-3} nm corresponds to six diodes so that the diode array does not degrade the resolution of the instrument. The scanning range was 0.3 nm.

The varying sensitivity of the individual diodes caused a structured pattern in the recorded spectra. To eliminate this, it was necessary to divide a measured spectrum by a reference spectrum without high-resolution features. This was accomplished by opening the entrance slit of the spectrograph. This degraded the resolution to a point where the absorption lines were no longer resolved.

For substances with broader absorption lines, a broadened absorption structure remains after the entrance slit is opened resulting in an overcompensation when dividing by the reference spectrum. This appears as an overshoot in the naphthalene spectra in Figures 2 to 4, but is of no consequence for the much narrower OH lines.

The spectra were digitally smoothed, which reduced the noise by about 50% while degrading the resolution by only 20% (Callies, 1988). The full wavelength range was covered by a succession of individual 0.3 nm spectra with overlapping wavelength intervals.

Solid substances under investigation were distributed on two 15–30 cm long, small aluminium plates, which were then inserted from either end into the measurement cell (length 135 cm). Liquid substances were placed in a saturator flask and the vapour was transferred into the measurement cell by a flow of nitrogen (50 ml/min).

In the case of naphthalene a separate cell of 1.22 m length was used. In order to obtain a uniform vapour pressure distribution in the cell, naphthalene crystals were distributed over its full length. A series of experiments showed that the naphthalene vapour pressure reached its equilibrium value within less than two hours. In order to minimize a possible formation of photolysis products, wavelengths below 300 nm were blocked by a glass filter (Schott WG 305).

Bromine oxide was produced in the reaction cell by photolyzing ethylbromide

(C_2H_5Br) in the presence of ozone:

$$C_2H_5Br \xrightarrow{h\nu} Br + C_2H_5 \quad (1)$$

$$Br + O_3 \longrightarrow BrO + O_2 \quad (2)$$

The cuvette was arranged in the center of four photolysis lamps (low pressure-mercury lamps, Philips TUV 40 W, length 1.20 m, photolysis wavelength 253.7 nm). To maintain constant temperature, a removable metal box was built around the four lamps and the cell. A N_2 flow was saturated with C_2H_5Br, and combined with an ozone flow produced by a pure oxygen-fed Siemens-type ozonizer. The BrO spectra were taken under the following conditions: Flow of C_2H_5Br/N_2 of 65 ml(stp)/min, O_2/O_3 flow of 350 ml/min (about 1% ozone in O_2). At a pressure of 120 mbar in the cell, those values correspond to an ozone concentration of 2.4×10^{16} molec/cm^3 and an C_2H_5Br concentration of 1.5×10^{18} molec/cm^3. The residence time in the cell was about eight seconds. Typical resulting BrO concentrations were 3×10^{12} molec/cm^3.

All substances used were purchased from E. Merck (Darmstadt, FRG) and had a purity between 95 and 96%. The concentration (except that of BrO) was determined by measuring the temperature and taking the corresponding vapour pressure from the literature (Landolt-Börnstein, 1960; *Handbook of Chemistry and Physics*, 1967–68; and Sonnefeld *et al.*, 1983).

In order to increase the vapour pressure of some of the species under investigation, the reaction cell was heated up to 77 °C. When liquid substances were investigated, the saturator flask was placed inside the heated metal box.

In case of 1- and 2-methylnaphthalene where vapour pressure data were lacking at the measurement temperature, they were extrapolated from tabulated values.

The BrO concentration in the cell was determined by simultaneously recording a BrO vibrational spectrum with a spectrograph of lower resolution (0.6 nm). The strongest vibrational band of BrO, the 7-0 band (at 338.3 nm) was utilized and its differential absorption cross-section was calculated from the literature (Cox *et al.*, 1982), where it was determined at a resolution of 0.55 nm ($\sigma' = (15.3 \pm 1.7) \times 10^{-18}$ cm^2/molec).

Applying Lambert-Beer's law, the differential absorption cross-section σ' of a single absorption line can be determined, provided that the concentration in the cuvette is known:

$$\sigma' = \frac{D'}{cl}, \quad (3)$$

where c = concentration,
l = length of the cell,
D' = $\ln(I_0'/I)$ = measured differential optical density,
I = light intensity at the center of the absorption line,
I_0' = light intensity as interpolated from either side of the line.

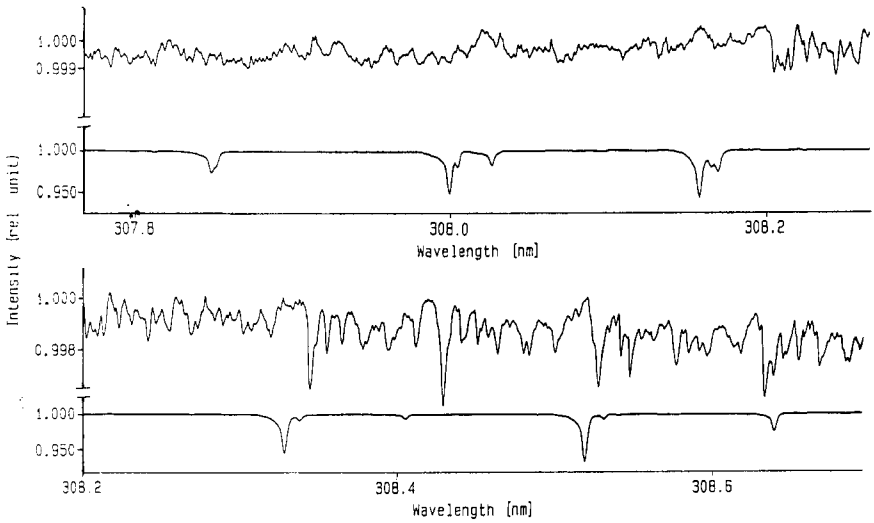

Fig. 1. BrO absorption spectrum (upper trace) in the wavelength region between 307.77 and 308.70 nm. The spectrum was recorded at a pressure of 120 mbar. The OH lines (lower trace) located in this interval are also shown for comparison. OH was generated by an acetylene air flame, therefore relative strength and width of the OH lines are different from those of atmospheric OH.

The minimum detectable differential optical density $D_{\min}$ is determined by the noise in the recorded spectrum. In order to determine $D_{\min}$, two spectra were taken with no absorbing substance in the cell at a spectrograph entrance slit widths of 12 and 170 μm.

Both spectra are treated in the same way as described above. In the resulting pure noise spectrum, the optical density of the largest structure found was taken as $D_{\min}$. For a series of experiments, $D_{\min}$ varied between 4×10^{-4} and 8×10^{-4}.

For determination of the exact absorption wavelength, the spectrograph was calibrated by an OH spectrum. OH radicals were produced in an acetylene air flame. In all figures, except, Figure 5, OH lines are shown as wavelength reference.

3. Results

3.1. *Bromine Oxide (BrO)*

Figure 1 shows the BrO spectrum in the wavelength interval between 307.77 and 308.70 nm. We were unable to find any BrO absorption lines significantly stronger than $D_{\min}$ in the wavelength region from 307.77 to 308.20 nm, which encompasses the $Q_1(2)$ and $Q_1(3)$ lines of the OH radical, those most commonly used for atmospheric OH detection. However, at longer wavelengths (308.2 to 308.7 nm), a large number of rotational lines of BrO exist. The strongest line in Figure 1 at 308.43 nm exceeded $D_{\min}$ about sixfold.

3.2. *Naphthalene ($C_{10}H_8$)*

In Figures 2 to 4 the positions of naphthalene and OH absorption lines are compared. Figures 2 and 3 show 0.15 nm regions around the $Q_1(2)$ and $Q_1(3)$ lines, respectively. In Figure 4, the interval ranging from 307.30 to 309.02 nm is represented. The strongest naphthalene absorption features occur very close to the OH lines.

Table I summarizes the differential absorption cross-sections of nine of the strongest naphthalene lines in the wavelength range 307.9 to 308.2 nm (see Figure 4). The cross-sections were measured at two different temperatures (t_1 = 22.5 °C and t_2 = 26.5 °C) and the corresponding naphthalene concentrations were calculated from the vapour pressures to be $c_1 = (2.24 \pm 0.23) \times 10^{15}$ molec/cm^3 and $c_2 = (3.30 \pm 0.33) \times 10^{15}$ molec/cm^3, respectively. The relatively large error is due to the uncertainty (± 1 °C) in the temperature determination in the reaction cell.

3.3. *Other Hydrocarbons*

In addition to naphthalene, we also studied a series of other hydrocarbons, mainly aromatics. As the light path during the recent series of tropospheric OH experiments at Jülich (Callies, 1988; Dorn *et al.*, 1988; Callies *et al.*, 1988) ran close to the roof (covered with roofing felt) of a building for a length of about 30 m, we completed this study by measurements of different samples of roofing felt.

All samples were analyzed for narrow-band absorption structures in the wavelength interval between 307.77 and 308.33 nm. In no case absorption structures exceeding our detection limit were found.

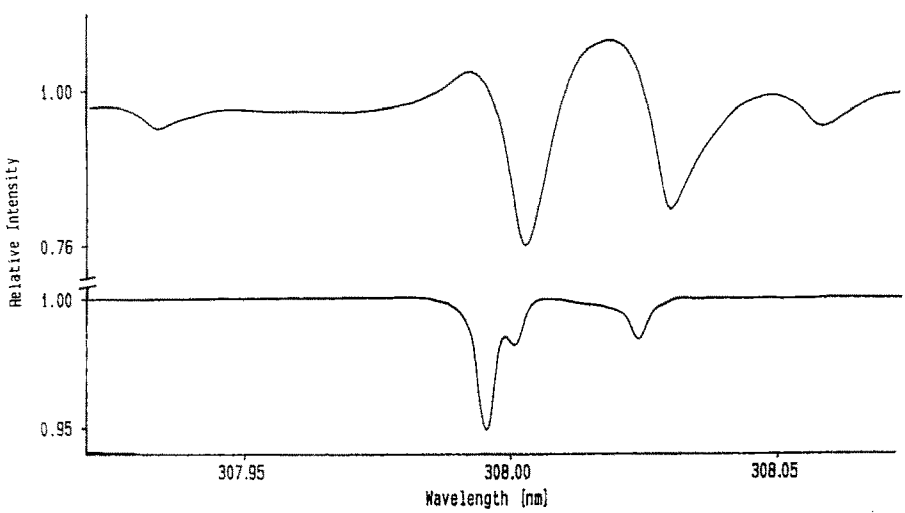

Fig. 2. Naphthalene absorption spectrum (upper trace) in the wavelength interval between 307.92 and 308.07 nm, in the vicinity of the $Q_1(2)$ line of the OH radical.

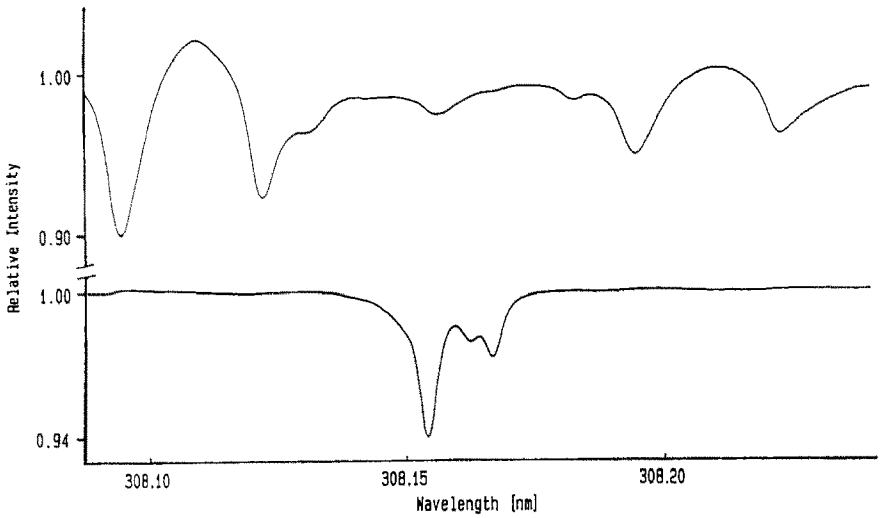

Fig. 3. Naphthalene absorption spectrum (upper trace) in the wavelength interval between 308.09 and 308.24 nm, in the vicinity of the $Q_1(3)$ and $P_1(1)$ lines of OH.

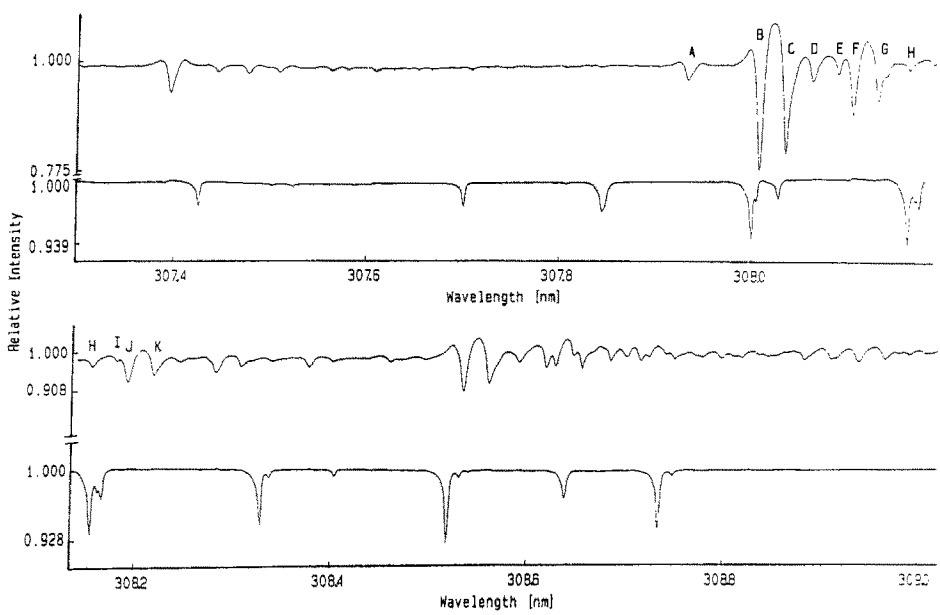

Fig. 4. Naphthalene absorption spectrum (upper trace) in the wavelength region between 307.30 and 309.02 nm. The OH lines (lower trace) located in this interval are also shown for comparison. OH radicals were generated by an acetylene air flame, therefore the relative strength and width of the OH lines are different from those of atmospheric OH. For lines A–H and line J the differential absorption coefficient σ' is determined.

Table I. Wavelength λ and differential absorption cross-section σ' of individual naphthalene absorption lines (line marking see Figure 4)

Absorption-line	Wavelength λ (nm)	$\sigma' \times 10^{20}$ (cm^2/molec)
A	307.934 ± 0.005	7.1 ± 1.4
B	308.002 ± 0.005	65.2 ± 15.3
C	308.030 ± 0.004	53.7 ± 11.3
D	308.057 ± 0.005	10.7 ± 2.2
E	308.082 ± 0.005	6.5 ± 1.8
F	308.097 ± 0.002	27.0 ± 4.9
G	308.125 ± 0.003	21.5 ± 2.7
H	308.156 ± 0.003	2.6 ± 0.5
J	308.192 ± 0.003	10.6 ± 1.7

Table II. Calculation of the differential absorption cross-section σ' from experimental data (taking the strongest feature (of optical density D'_{min}) as a real absorption line, upper limits (with exception of $C_{10}H_8$) for the diff. abs. cross-sections σ' were calculated in the wavelength interval between 307.77 and 308.33 nm.)

Absorbing substance	Temperature [°C]	Concentration (molec/cm^3)	$D'_{min} \times 10^4$	σ' (position) (cm^2/molec (nm))
naphthalene $C_{10}H_8$	22.5	2.2×10^{15}	1.8×10^3	6.5×10^{-19} (308.002)
1-methylnaphthalene $C_{11}H_{10}$	22	2.5×10^{16}	6.0	$\leq 1.8 \times 10^{-22}$ (308.223)
2-methylnaphthalene $C_{11}H_{10}$	60	3.2×10^{16}	7.0	$\leq 1.6 \times 10^{-22}$ (308.016)
1-naphthol $C_{10}H_8O$	24	–	5.8	–
2-naphthol $C_{10}H_8O$	63	–	7.5	–
anthracene $C_{14}H_{10}$	20	1.1×10^{11}	5.0	$\leq 3.7 \times 10^{-17}$ (308.121)
phenanthrene $C_{14}H_{10}$	22	2.4×10^{12}	5.4	$\leq 1.9 \times 10^{-18}$ (308.041)
glyoxal $C_2H_2O_2$	77	7.6×10^{17}	6.5	$\leq 6.3 \times 10^{-24}$ (308.204)
benzaldehyde C_7H_6O	25	3.0×10^{16}	5.0	$\leq 1.3 \times 10^{-22}$ (307.958)
propionaldehyde C_3H_6O	22	1.1×10^{19}	4.1	$\leq 2.8 \times 10^{-25}$ (307.970)
pyridine C_5H_5N	24	6.0×10^{17}	4.6	$\leq 5.7 \times 10^{-24}$ (308.178)
toluene C_7H_8	27	1.1×10^{18}	5.7	$\leq 4.0 \times 10^{-24}$ (308.246)
xylene $C_6H_4(CH_3)_2$	26	2.8×10^{17}	7.3	$\leq 1.9 \times 10^{-23}$ (308.037)
tar	67	–	4.0	–
roofing felt	71	–	5.5	–
roofing felt I	70	–	6.7	–
roofing felt II	70	–	5.9	–
roofing felt III	70	–	5.8	–

The sample concentrations were calculated from literature data of the vapour pressure as mentioned before. Together with the minimum detectable optical densities D_{min} upper limits for the individual differential absorption cross-sections σ' were calculated. The results are summarized in Table II. With the exception of anthracene and phenanthrene, the cross-sections are below 10^{-22} cm^2. High values

for the differential absorption cross-section σ' for these two PAHs are the results of their low vapour pressure which does not imply absorption transitions of this strength.

4. Discussion

Because, out of all investigated substances, only BrO and naphthalene show a rotational structure within the wavelength region under study, the discussion will be restricted to the latter two molecules.

4.1. *BrO Spectra*

BrO shows a vibrational band transition (15-0) with its zero-line at 306.96 nm (Barnett *et al.*, 1981). Because the rotational structure of this vibrational transition ($A^2\Pi_{3/2} \leftarrow X^2\Pi_{3/2}$) is degraded to longer wavelengths with its band head near the band origin, BrO may be a potential OH interference.

As can be seen in Figure 1, however, the rotational structure only begins at $\lambda > 308.2$ nm and by determining the BrO concentration as described above, we obtained $\sigma'_1 < (1.5 \pm 0.2) \times 10^{-18}$ cm^2/molec in the wavelength interval 307.75 to 308.2 nm and $\sigma'_2 = (10 \pm 1.5) \times 10^{-18}$ cm^2/molec for the strongest observed line at 308.43 nm. Therefore, BrO would not interfere with OH measurements as long as the strongest OH bands ($Q_1(2)$, $Q_1(3)$ and $P_1(1)$) are employed.

To our knowledge, there are no measurements of the tropospheric BrO concentration. In the stratosphere, however, especially in polar regions, BrO concentrations can be appreciable (total column densities of the order of several 10^{14} cm^{-2} have been reported (Carroll *et al.*, 1989; Wahner *et al.*, 1990)). There, it is believed to significantly contribute to the catalytic ozone destruction (Hills *et al.*, 1987).

Using the narrow-band absorption lines, BrO vertical-column densities could be measured by observing direct or scattered sunlight. High-resolution detection of BrO could overcome some of the difficulties of the low-resolution technique used up to now (Caroll *et al.*, 1989; Wahner *et al.*, 1990). This especially relates to less interference by Fraunhofer lines and the lack of absorptions of trace gases like O_3 and NO_2, which are known to have virtually no highly resolved band structure at the wavelength region of interest (Hübler *et al.*, 1984).

Assuming a BrO vertical column density of 10^{14} cm^{-2} and an airmass factor of 10, this would result in a differential optical density D' of 10^{-2}, if the strongest BrO line at 308.43 nm were used.

4.2. *Naphthalene Spectra*

Naphthalene showed narrow-band absorption lines in the wavelength region around the $Q_1(2)$ and the $Q_1(3)$ line of the OH radical and must, therefore, be regarded as a possible interference to atmospheric OH absorption measurements.

Part of our spectrum can be compared with a naphthalene spectrum recorded by Hollas and Thakur (1971) (Figure 5), who used a spectrograph with higher resolution. Therefore, they were able to resolve the rotational features in more detail than we could. In the wavelength interval between 308.07 and 308.30 nm, the lines F, G, J and K (see Figure 4) have the same wavelength position (see figure 5). However, we observed lines H and I at longer wavelengths compared to Hollas, although the distance between both lines is equal. The reason for this discrepancy is unknow. In addition, there is a difference in the strength of the absorption lines, but this is likely due to the fact that the two spectra were recorded at different temperatures (Hollas's 60°–100 °C, this work 22°–26 °C).

The strongest line absorption of naphthalene (line 'B' at 308.002 nm, $\sigma' = 6.5 \times 10^{-19}$ cm^2/molec (see Table I)) is about a factor of 200 weaker than the OH $Q_1(2)$-line ($\sigma' = 1.3 \times 10^{-16}$ cm^2). Thus, in order to cause a noticeable interference, atmospheric naphthalene concentrations must be about a factor of 200 higher than the OH concentration. For instance, 15 ppt of naphthalene will give an absorption line similar in strength to that due to 2×10^6 OH cm^{-3}.

Concentration measurements of cyclic aromatic hydrocarbons in the atmosphere have been carried out in the last few years. For naphthalene, such measurements were performed in rural or coastal as well as in highly industrialized regions

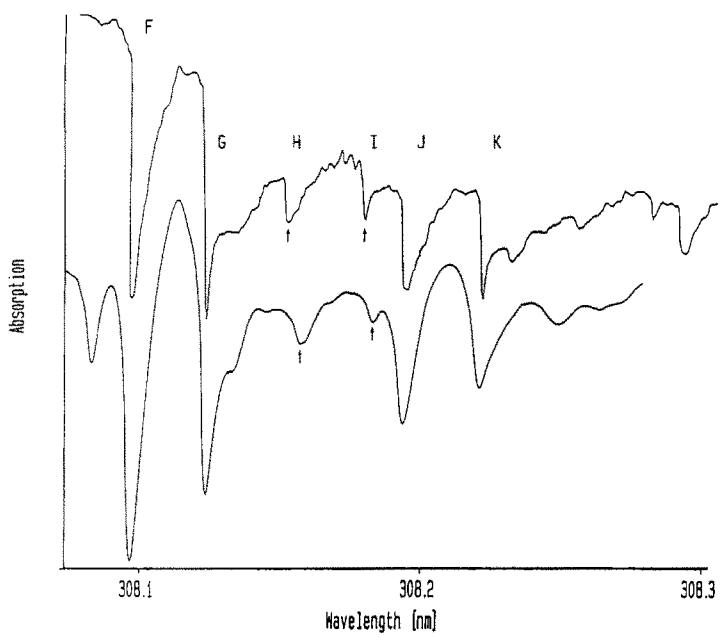

Fig. 5. Comparison of naphthalene absorption spectra in the wavelength range between 308.07 and 308.30 nm. The upper trace shows the spectrum recorded by Hollas and Thakur (1971) at higher resolution. The wavelength positions of the lines match within the error limits, with the exception of two lines (arrows) in the center of the spectrum. Inexplicably, they are shifted to shorter wavelengths in Hollas's spectrum, although the distance between them is equal in both spectra.

(Arey *et al.*, 1989; Graedel, 1978; Graedel *et al.* 1986; Krustulovic *et al.*, 1977; Thrane, 1987, 1988).

The mixing ratios range from 0.01 ppt (Krustulovic *et al.*) in the rural coastal area of Saunderstown (Rhode Island) up to 1.2 ppb (Arey *et al.*) in Glendora (20 km northeast from Los Angeles) during a photochemical air pollution period. Arey *et al.*'s measurements showed a diurnal variation of naphthalene with higher concentrations at night. On the average, they found an about 39% lower daytime concentration, which was attributed to the gas-phase reaction of naphthalene with OH radicals.

Naphthalene is a product of combustion processes so it is quite likely that considerable amounts of naphthalene could be present in the air of Jülich because the town is surrounded by coal-fired power plants and lies close to the highly industrialized Rhine-Ruhr valley.

In Jülich, OH spectra were recorded with a tunable dye laser as a light source on 5 July 1987 (Callies, 1988). The frequency doubled output ($\lambda = 308$ nm) had a FWHM of 0.15 nm, so that it was only possible to record spectra either in the wavelength region around the $Q_1(2)$ or the $Q_1(3)$ line (line separation 0.15 nm). Because the differential absorption cross-section of naphthalene in the vicinity of the $Q_1(3)$ line (308.15 nm) is about a factor of 3 weaker than at 308 nm, we restrict our discussion to air spectra at 308 nm.

The detection limit for naphthalene, as far as our OH measurements in Jülich (1987) are concerned, was calculated with the minimum detectable optical density of 1.5×10^{-4} for atmospheric measurements, a light path length of 5.8 km and the strongest naphthalene line (line 'B') to a value of about 4×10^8 molec/cm^3 (≈ 15 ppt).

On 5 July, 14 single spectra with integration times up to 20 min were recorded, in which we attempted to detect naphthalene lines. In addition, we averaged spectra over time intervals of about two to three hours to extract weaker naphthalene absorptions. Careful re-examination of these spectra shows the possible presence of the two strongest naphthalene lines 'B' and 'C', whereby line 'C' seems to be superimposed by another absorption and so it can hardly be seen as a single line (see Figure 6).

The optical density of line 'B' in the naphthalene spectrum (Figure 6) fitted and scaled to the sum spectra of the whole day (third spectrum in Figure 6) corresponds to a mixing ratio of about 30 ppt. Due to the low SNR, this value has to be regarded as an upper limit for the naphthalene mixing ratio.

Figure 6 shows that naphthalene does not directly interfere with the OH lines, but the close neighborhood of some naphthalene and OH lines (chiefly line 'B' and $Q_1(2)$ line) makes it possible to confuse the lines. This again stresses how necessary it is to record a wider spectral range for the detection of OH, as was made possible by the introduction of the photodiode array in our OH spectrometer.

Since naphthalene mixing ratios in excess of 60 ppt are possible in urban areas (e.g. Arey *et al.*, 1989), the knowledge of the naphthalene spectrum in a wider

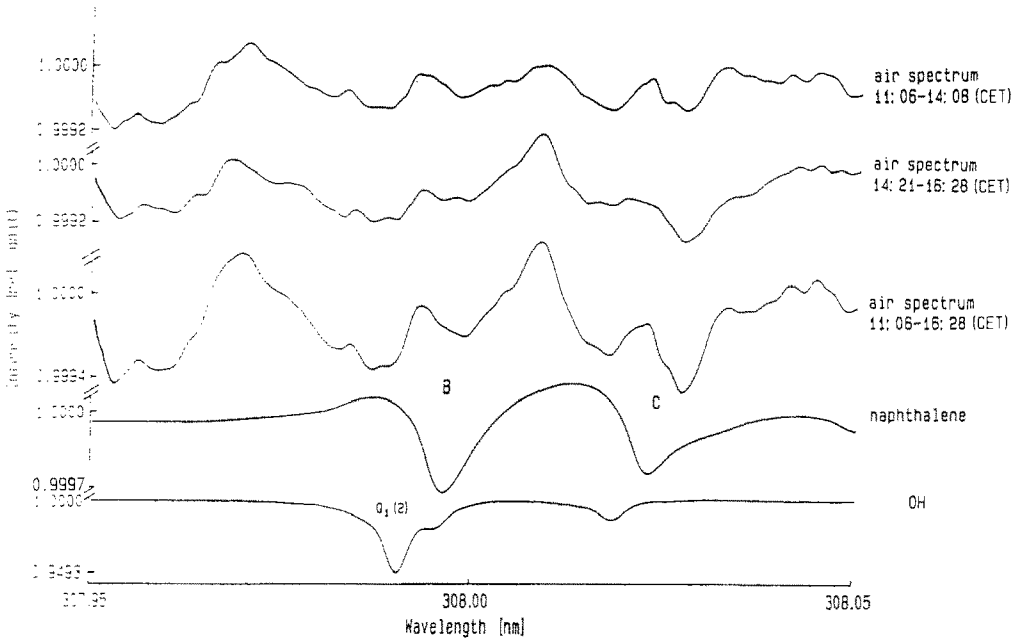

Fig. 6. Air spectra (SO_2 interference already subtracted) recorded in Jülich on 5 July 1987 in the wavelength interval between 307.95 and 308.05 nm. The naphthalene spectrum is fitted and scaled to the sum spectrum (11 : 06–16 : 28). For comparison OH lines measured in a flame are shown to indicate their spectral position.

wavelength-interval makes the high-resolution absorption spectroscopy to a technique, which allows the detection of atmospheric naphthalene with high sensitivity and selectivity. Moreover, the naphthalene lines 'B' and partly 'C' may be the reason for two of the unknown structures in the air spectra on 5 July (see Figure 6).

References

Arey, J., Atkinson, R., Zielinska, B., and McElroy, P. A., 1989, Diurnal concentrations of volatile polycyclic aromatic hydrocarbons and nitroarenes during a photochemical air pollution episode at Glendora, CA, *Environ. Sci. Technol.* **23**, 321–327.

Barnett, M., Cohen, E. A., and Ramsay, R. D., 1981, The $A^2\Sigma_i - X^2\Pi_i$ absorption spectrum of BrO, *Can. J. Phys.* **59**, 1908–1916.

Callies, J., Dorn, H.-P., Platt, U., and Ehhalt, D. H., 1988, Tropospheric OH concentration measurements by laser long path absorption spectroscopy, *Proc. Quadrennial Ozone Symposium, Göttingen*.

Callies, J., 1988, Absorptionsspektroskopischer Nachweis von Hydroxyl-Radikalen in der Troposphäre, Thesis, Universität Köln.

Carroll, M. A., Sanders, R. W., Solomon, S., and Schmeltekopf, A., 1989, Visible and near UV spectroscopy at McMurdo Station Antarctica. 6. Observation of BrO, *J. Geophys. Res.* **94**, 16,633–16,638.

Cox, R. A., Sheppard, D. W., and Stevens, M. P., 1982, Absorption coefficients and kinetics of the BrO radical using molecular modulation, *J. Photochem.* **19**, 189–207.

Dorn, H.-P., Callies, J., Platt, U., and Ehhalt, D. H., 1988, Measurement of tropospheric OH concentrations by laser long path absorption spectroscopy, *Tellus* **40B**, 437–445.

Graedel, T. E., 1978, *Chemical Compounds in the Atmosphere*, Academic Press, New York.

Graedel, T. E., Hawkins, D. T., and Claxton, L. D., 1986, *Atmospheric Chemical Compounds*, Academic Press, New York.

Handbook of Chemistry and Physics, 1967–1968, The Chemical Rubber Co., D-142, 48th edn., p. D-142.

Hills, A. J., Cicerone, R. J., Calvert, J. C., and Birks, J. W., 1987, Kinetics of the BrO + ClO reaction and implication for stratospheric ozone, *Nature* **328**, 405–408.

Hollas, J. M. and Thakur, S. N., 1971, Rotational band contour analysis in the 3120 Å system of naphthalene, *Molec. Phys.* **22**, 203–212.

Hübler, G., Perner, D., Platt, U., Toennissen, A., and Ehhalt, D. H., 1984, Groundlevel OH Radical Concentration: New Measurements by Optical Absorption, *J. Geophys. Res.* **89**, 1309–1319.

Krustulovic, A. M., Rosie, D. M., and Brown, P. R., 1977, Distribution of some atmospheric polynuclear aromatic hydrocarbons, *American Laboratory* **9**, 11–18.

Landolt-Börnstein, 1960, *Zahlenwerte und Funktionen, II.* Band 2. Teil, 6th edn., Springer-Verlag, Heidelberg, Berlin.

Sonnefeld, W. J., Zoller, W. H., and May, W. E., 1983, Dynamic coupled-column liquid chromatographic determination of ambient temperature vapor pressures of polynuclear aromatic hydrocarbons, *Anal. Chem.* **55**, 275–280.

Thrane, K. E., 1987, Ambient air concentrations of polycyclic aromatic hydrocarbons, fluoride, suspended particles and particulate carbon in areas near aluminium production plants, *Atmos. Environ.* **21**, 617–618.

Thrane, K. E., 1988, Application of air pollution models: a comparison of different techniques for estimating ambient air pollution levels and source contributions, *Atmos. Environ.* **22**, 587–594.

Wahner, A., Callies, J., Dorn, H.-P., Platt, U., and Schiller, C., 1990, Near UV atmospheric absorption measurements of column abundances during airborne arctic stratospheric expedition, January–February 1989: 3. BrO observations, *Geophys. Res. Lett.* **17**, 517–520.